

Supplementary Materials: Reconfigurable Radiation Angle Continuous Deflection of All-dielectric Phase-change V-shaped Antenna

Ping Tang ¹ , Qiao Tao ¹, Shengde Liu ², Jin Xiang ³, Liyun Zhong ^{1,*} and Yuwen Qin ¹

1. Electromagnetic Field Mode

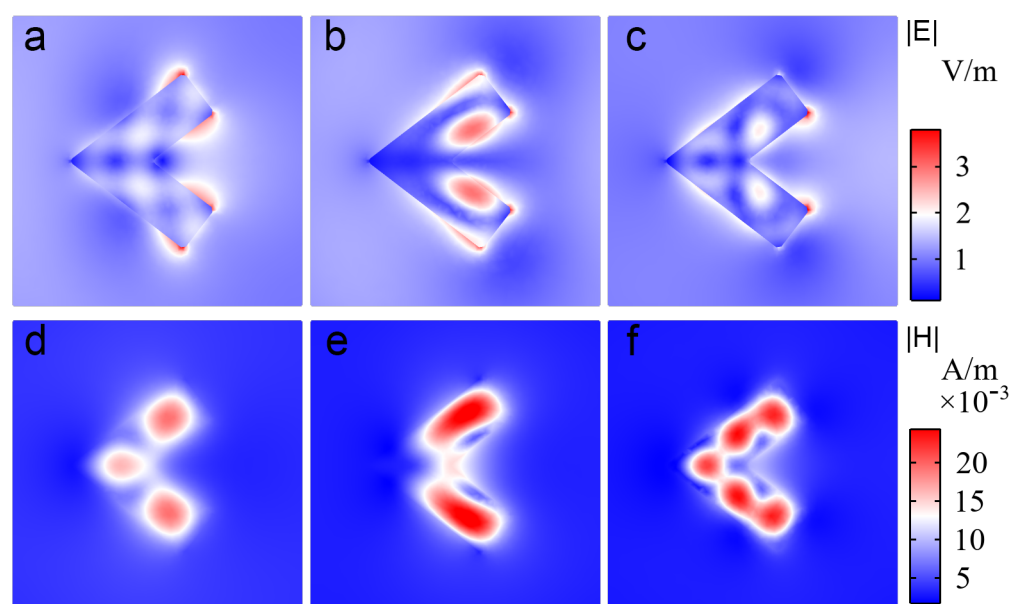


Figure S1. (a–c) Electric ($|E|$) and (d–f) magnetic ($|H|$) field distributions in the xy -plane of the V-shaped phase-change antenna at $3.6 \mu\text{m}$ wavelength with crystallinity of 20%, 50%, and 80%, respectively.

2. Amorphous and Crystalline V-shaped Phase-change Antennas

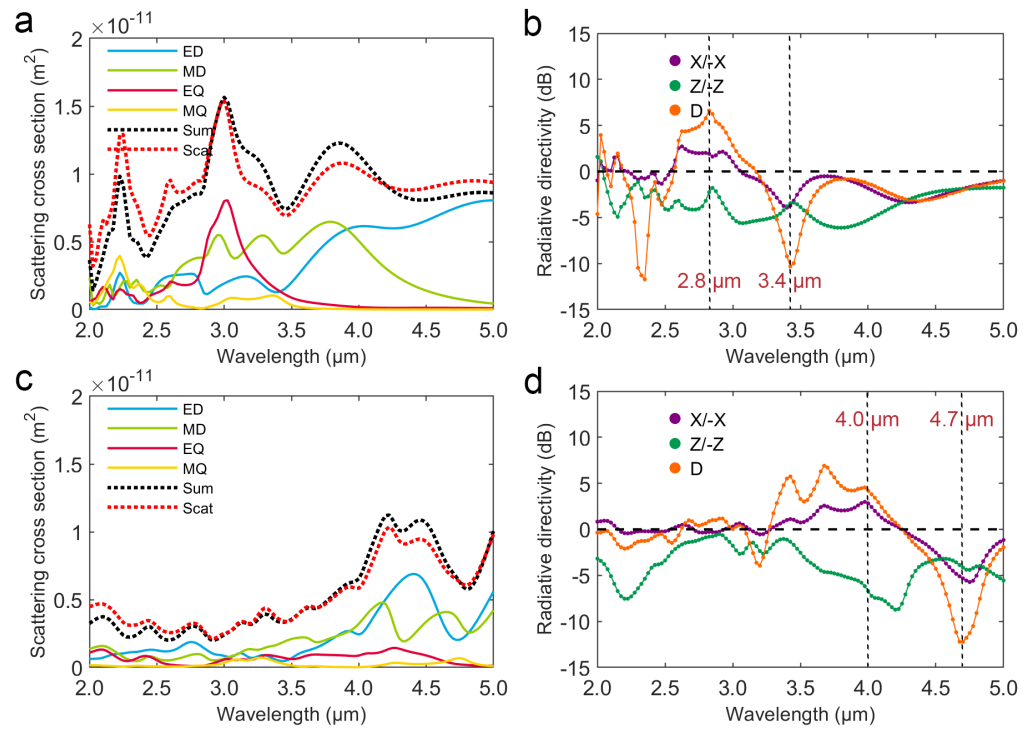


Figure S2. Multipole scattering cross sections and directivities of the V-shaped phase-change antenna in 2.0 to 5.0 μm wavelength range: **(a, c)** Scattering cross sections of ED, MD, EQ, MQ, their summation (Sum) and the total scattering cross sections calculated according to scattering filed (Scat) at the crystallinity of 0% and 100%, respectively; **(b, d)** Directivities of x -axis positive and negative (X/-X), z -axis positive and negative (Z/-Z), and the specific angle and window (D: $\theta_0=135^\circ$, $\delta=10^\circ$) at the crystallinity of 0% and 100%, respectively.

3. Far-field Radiation Patterns of Unit Multipole Scattering Moment

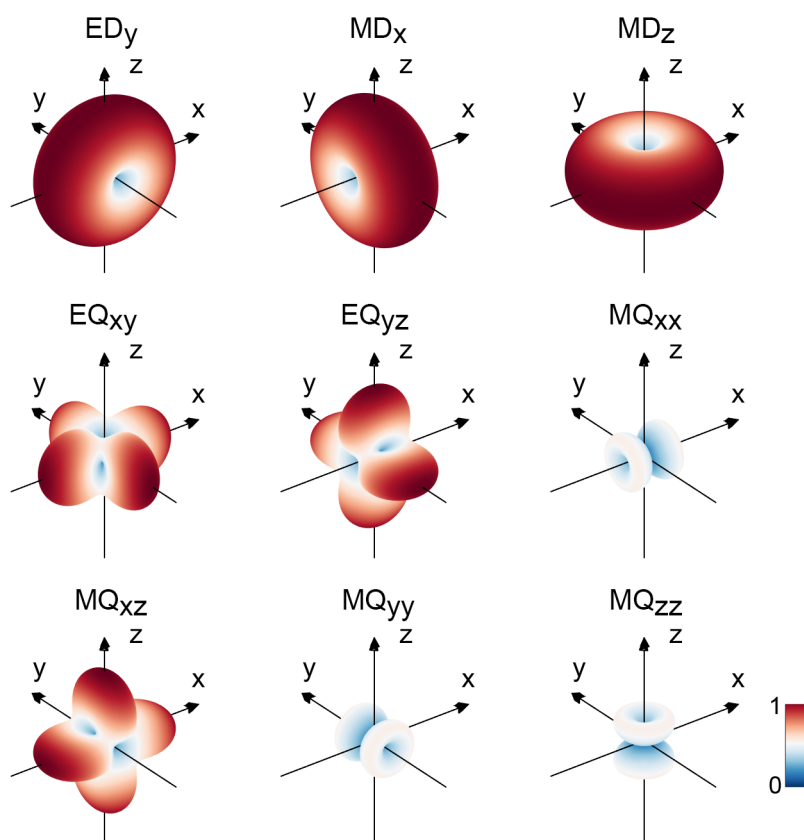


Figure S3. Far-field radiation patterns of unit ED_y , MD_x , MD_z , EQ_{xy} , EQ_{yz} , MQ_{xx} , MQ_{xz} , MQ_{yy} , and MQ_{zz} , respectively.

4. Interference Far-field Radiation of Unit Multipole Moments

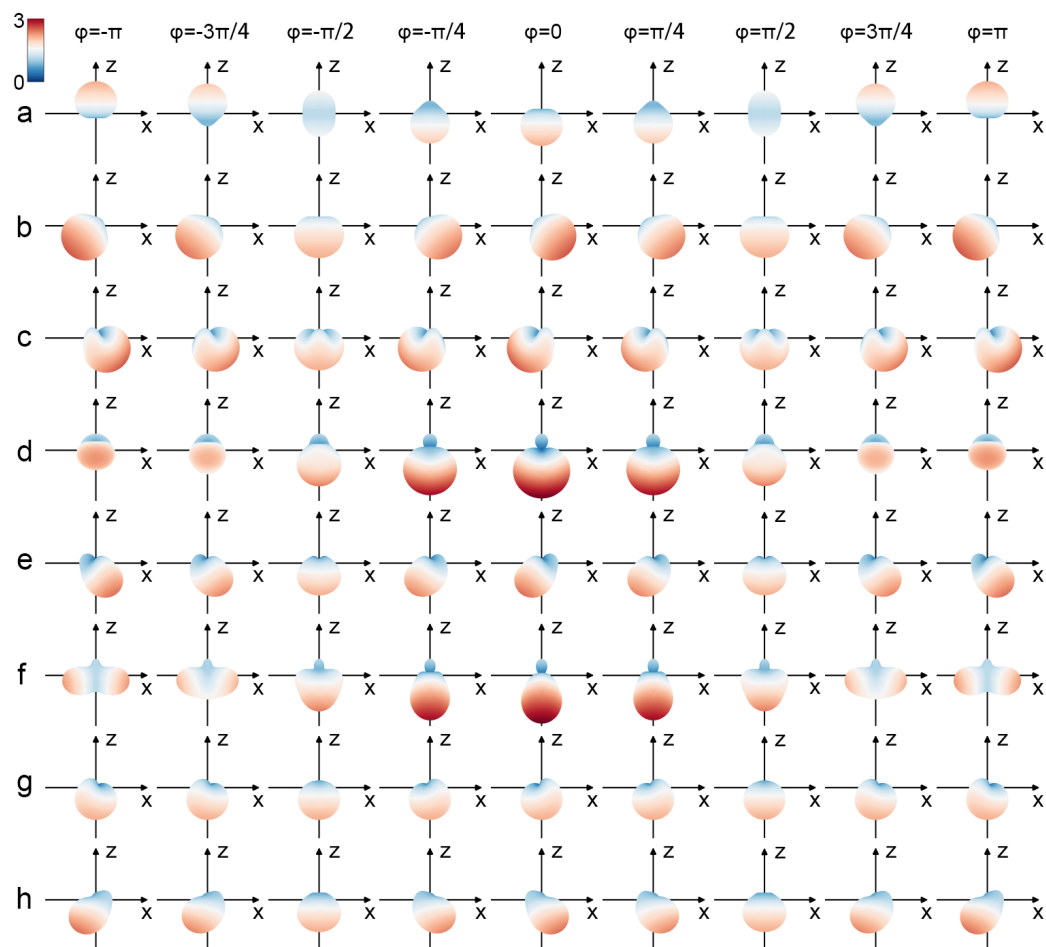


Figure S4. Interference far-field radiation patterns of the unit multipole moments with different phase differences: Far-field radiation patterns of (a) $ED_y + \exp(i\varphi)MD_x$, (b) $ED_y + MD_x + \exp(i\varphi)MD_z$, (c) $ED_y + MD_x + \exp(i\varphi)EQ_{xy}$, (d) $ED_y + MD_x + \exp(i\varphi)EQ_{yz}$, (e) $ED_y + MD_x + \exp(i\varphi)MQ_{xx}$, (f) $ED_y + MD_x + \exp(i\varphi)MQ_{xz}$, (g) $ED_y + MD_x + \exp(i\varphi)MQ_{yy}$, and (h) $ED_y + MD_x + \exp(i\varphi)MQ_{zz}$.

The interference far-field radiation patterns of unit moments with different phase difference are shown in Figure S4. It can be seen that MD_x with different phase angle mainly affects the backward and forward scattering in the z -direction (Figure S4a). The calculated interference phase difference between MD_x and ED_y (see Figure 5b) varies between $-\pi/2$ and $\pi/2$ in crystallinity 0% to 100% range, so its main contribution is forward scattering to the $-z$ direction. In order to clarify the contribution of other unit multipole moments to the interference far-field, we analyzed the interference far-field radiation of $ED_y + MD_x + \exp(i\varphi)MD_z$, $ED_y + MD_x + \exp(i\varphi)EQ_{xy}$, $ED_y + MD_x + \exp(i\varphi)EQ_{yz}$, $ED_y + MD_x + \exp(i\varphi)MQ_{xx}$, $ED_y + MD_x + \exp(i\varphi)MQ_{xz}$, $ED_y + MD_x + \exp(i\varphi)MQ_{yy}$, and $ED_y + MD_x + \exp(i\varphi)MQ_{zz}$, and the results are shown in Figure S4b–S4h, respectively. Distinctly, the MD_z , EQ_{xy} , MQ_{xx} , and MQ_{zz} deflect the interference far-field radiation direction; On the contrary, the contributions of EQ_{yz} and MQ_{xz} to the interference far-field radiation are symmetric about the yz -plane; And the intrinsic far-field radiation mode of unit MQ_{yy} (Figure S3) is none in xz -plane, so that its influence on D directivity can be ignored. Above results are consistent with the discussion based on Eq. 23 in the main text. Note that: 1) MQ_{xx} and MQ_{zz} belong to the third-order mode and the modulus of calculated scattering coefficient $\alpha_{MQ_{xx}}$ and $\alpha_{MQ_{zz}}$ are small relative to that of α_{MD_z} and $\alpha_{EQ_{xy}}$ (see Figure 4a), so as the contributions of MQ_{xx} and MQ_{zz} to the interference far field is relatively little; 2) It can be seen from Figure S4 that the intrinsic far field radiation patterns of unit MQ_{xx} and

MQ_{zz} are smaller than these of MD_z and EQ_{xy} , so MQ_{xx} and MQ_{zz} have a relatively minor impact. As a result, MD_z and EQ_{xy} make minor contributions to the radiation deflection while MD_z and EQ_{xy} are the key moments to the deflection of direction and make the major contributions to the D directivity. The detailed contributions of ED_y , MD_x , MD_z , and EQ_{xy} to the interference far-field radiation are discussed in the main text.

5. Directivity of Interference Far-field Radiation with Minor Contributions

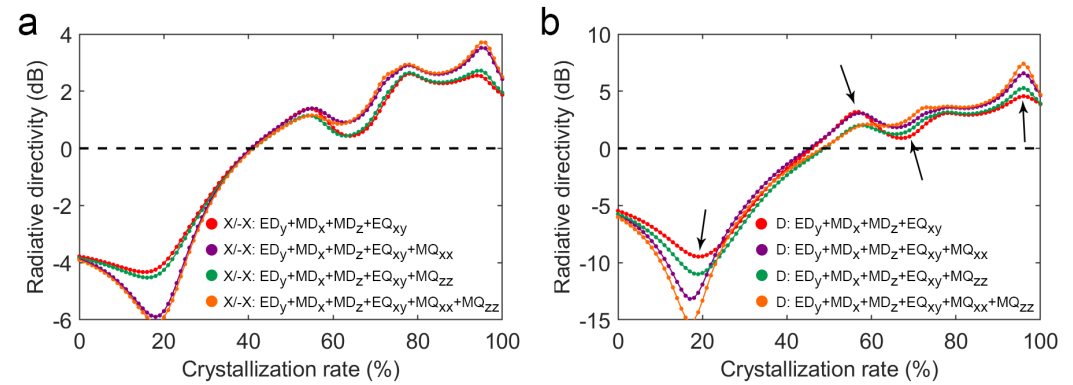


Figure S5. Directivities of interference far-field radiation according to the complex coefficients of major (ED_y , MD_x , MD_z , and EQ_{xy}) and minor (MQ_{xx} and MQ_{zz}) multipole moments at $3.6 \mu\text{m}$ wavelength: (a) X/-X directivity as a function of crystallinity; (b) D directivity as a function of crystallinity.

6. Effect of Geometric Angle on Directivity of V-shaped Phase-change Antenna

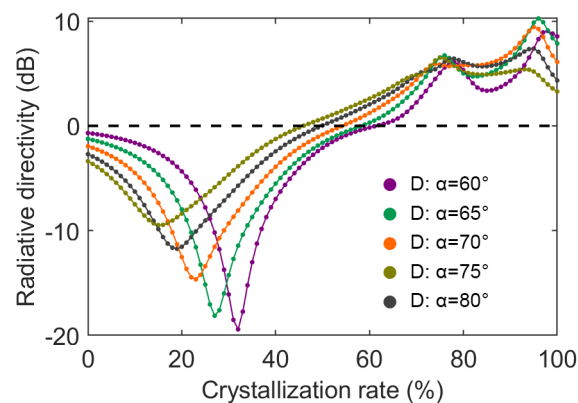


Figure S6. D directivities of V-shaped phase-change antenna with different geometric angles (α in Figure 1a), including $\alpha=60^\circ$, $\alpha=65^\circ$, $\alpha=70^\circ$, $\alpha=75^\circ$, and $\alpha=80^\circ$.